Maximizing Acetyl-CoA Output by Genetically Engineering *E. coli* for the Overall Output of the Bioplastic PHB

A Technical Report submitted to the Department of Biomedical Engineering

Presented to the Faculty of the School of Engineering and Applied Science

University of Virginia • Charlottesville, Virginia

In Partial Fulfillment of the Requirements for the Degree

Bachelor of Science, School of Engineering

Julia Zhi-Yi Yao

Spring, 2022.

Technical Project Team Members

Hannah Towler

Sang-Hoon Park

Xin Chen

Tammy Tran

Thomas Nguyen

On my honor as a University Student, I have neither given nor received unauthorized aid on this assignment as defined by the Honor Guidelines for Thesis-Related Assignments

Mark Kester, Department of Pharmacology, Biomedical Engineering, Molecular Physiology and Biophysics

Keith Kozminski, Doctor of Philosophy, Departments of Biology and Cell Biology

Maximizing Acetyl-CoA Output by Genetically Engineering *E. coli* for the Overall Output of the Bioplastic PHB

Author(s):

Hannah Towler
Sang-Hoon Park
Julia Yao
Xin Chen
Tammy Tran
Thomas Nguyen

University of Virginia, Department of Biomedical Engineering Spring 2022

Faculty Advisor(s):

Mark Kester, Department of Pharmacology, Biomedical Engineering, Molecular Physiology and Biophysics

Keith Kozminski, Doctor of Philosophy, Departments of Biology and Cell Biology

Word Count: 4,281
Figure(s): 7
Table(s): 0
Equation(s): 5
Supplement(s): 5
Reference(s): 17

Approved:_____ Date: 05/06/2022
Mark Kester, Department of Biomedical Engineering

Maximizing Acetyl-CoA Output by Genetically Engineering *E. coli* for the Overall Output of the Bioplastic PHB

Hannah Towler[a]. Sang-Hoon Park[b], Julia Yao[c], Xin Chen[d], Tammy Tran[e], Thomas Nguyen[f]

[a] Hannah Towler; Biomedical Engineering Undergraduate, UVA
[b] Sang-Hoon Park; Biomedical Engineering Undergraduate, UVA
[c] Julia Yao; Biomedical Engineering Undergraduate, UVA
[d] Xin Chen; Biomedical Engineering Undergraduate, UVA
[e] Tammy Tran; Biomedical Engineering Undergraduate, UVA
[f] Thomas Nguyen; Biomedical Engineering Undergraduate, UVA

Abstract

Unsustainable production, consumption, and disposal of single-use plastics have prompted the adoption of alternative plastics that impose less of an environmental burden. Bioplastics, plastics that are biobased and/or biodegradable, significantly offset waste accumulation in contrast to conventional plastics. Our sponsor, Transform LLC, is currently developing a modified strain of *Escherichia coli* (*E. coli*), which includes two plasmids (*sty* and *pha*) giving it the ability to utilize styrofoam as its carbon feedstock and synthesize PHB. The metabolic pathways encoded by the *sty* and *pha* plasmids are bridged by the central metabolite acetyl-CoA, which serves as the main precursor to PHB production. The ackA-pta pathway is a nonessential pathway that diverts acetyl-CoA from PHB production. Here, we propose the deletion of the ackA and pta genes to reduce loss of carbon flux towards acetate production and increase the intracellular concentration of acetyl-CoA. These gene knockouts were performed on the *E. coli DH5α* cell line through recombineering with CRISPR-Cas9 coupled with lambda red phage display. Acetyl-CoA concentrations were quantified fluorometrically and normalized with their respective cell culture wet weight to result in 0.041±0.006, 0.027±0.007, and 0.039±0.007 μM/mg for ΔackA, Δpta, and control, respectively. ΔackA resulted in significantly lower acetyl-CoA concentrations than both control and Δpta (p<0.05). In addition, perturbations performed on the published iML1515 *E. coli* K-12 MG1655 genome-scale metabolic model (GEM) inform additional gene deletions that could further improve upon these results, including ΔsucC and ΔsucD. These additional knockouts show potential in coupling PHB production to cell growth with glucose substrate, guaranteeing a baseline rate of PHB production provided that cells are actively growing.

Keywords: acetyl-CoA, PHB, ackA-pta pathway, *Escherichia coli*, carbon flux, Genome-Scale Modeling (GEM), CRISPR/Cas9, lambda red phage display, recombination, gene knockouts, acetate, bioplastics

Introduction

Each year, more than 380 million tons of plastic are produced globally, of which about half are single-use plastics [1]. Single-use plastics are readily disposed of immediately after use and end up as pollutants contributing to an insurmountable plastic waste crisis. Polyhydroxybutyrate (PHB), a non-toxic, biodegradable plastic, has been steadily gaining traction as a sustainable alternative to petrochemical derived plastics. Because PHB is a naturally occurring (microbially produced) bioplastic, it can be easily degraded in virtually any microbially active environment, ultimately reducing plastic accumulation in landfills [2].

However, one of the primary barriers hindering PHB as a competitive alternative to conventional petrochemical plastics are the lower production yields which contribute to higher manufacturing costs. The difficulty of acquiring an inexpensive carbon source that is also coupled to *E. coli* growth contributes to the cost of PHB being approximately 16 times the price of polypropylene (PE)–a synthetic polymer used in a variety of applications [3]. Previous studies have focused on using glucose and other agro-industrial products as carbon feedstocks, which creates competition for arable land and increases the carbon footprint from agricultural emissions [4]. In order to tackle this problem, companies have started

pioneering metabolically engineered microorganisms that can produce bioplastics from inexpensive carbon waste sources [5].

Several microbial strains have currently been shown to produce and accumulate intracellular polymeric granules of PHB. Our sponsor, Transfoam LLC, is currently developing a modified strain of *E. coli* K-12 MG1655 that is not only able to synthesize PHB, but also utilize styrene (monomer of styrofoam) as its carbon source. This was achieved with the inclusion of the *sty* plasmid from *Pseudomonas putida* (*P. putida*), which encodes for enzymes that convert styrene to phenylacetic acid, and the *pha* plasmid from *Cupriavidus necator* (*C. necator*), which encodes for enzymes that convert acetyl-CoA into PHB. In these cells, the metabolic pathways encoded by the *sty* and *pha* plasmids are bridged by the central metabolite acetyl-CoA, which serves as the direct precursor for the PHB production pathway. As such, this work primarily aims to increase acetyl-CoA concentrations within *E. coli*.

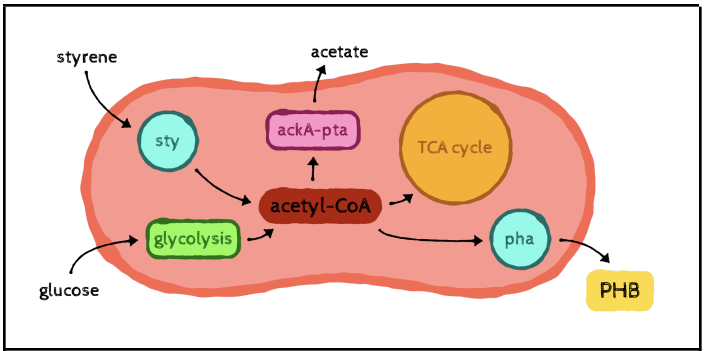

Fig. 1. Overview of pathways explored in our bacteria. Blue circles indicate inclusion of sty and pha plasmids in bacteria. In order to increase acetyl-CoA concentrations and subsequently PHB yields, we investigate glucose uptake through glycolysis, acetate production through ackA-pta, and metabolite and energy production through the TCA cycle.

While many factors influence acetyl-CoA concentrations in the cell, we have focused on investigating three of the most prominent: (i) the primary carbon source cells will be grown on; (ii) the ackA-pta pathway responsible for producing acetate from acetyl-CoA; and (iii) the tricarboxylic acid (TCA) cycle which consumes acetyl-CoA to synthesize essential metabolites and aid in aerobic respiration (Fig. 1). For the purpose of improving PHB yields, carbon feedstocks for microbial biofactories must use metabolites that are favored by the cell to improve metabolic efficiency and reduce associated manufacturing costs. While the use of styrene allows for the simultaneous recycling of conventional plastics and production of PHB, its degradation in the cell solely depends on the pathway encoded by *sty* and excludes glycolysis, a core metabolic pathway that allows the cell to produce energy in anaerobic conditions. Alternatively, glucose is the naturally preferred feedstock of *E. coli* and has been used extensively as a general feedstock. When grown in favorable conditions, glucose allows cells to access and utilize their metabolisms to their fullest extent, suggesting improved PHB yields in cells in comparison to styrene. As both carbon sources notably lead to the production of acetyl-CoA and subsequently PHB in our bacteria, the first component of our work seeks to quantify improvements in PHB yield using *in silico* metabolic modeling for growth on each carbon source. The results obtained here lend insight for providing cells ideal extracellular conditions for PHB production.

A major component responsible for acetyl-CoA consumption in the central *E. coli* metabolism is the ackA-pta pathway, which funnels acetyl-CoA into acetate production. Composed of acetyl-CoA kinase (*ackA*) and phosphate acetyltransferase (*pta*), this metabolic pathway is hypothesized to result from an imbalance in the cell's ability to produce and use acetyl-CoA, and serves as a way for the cell to store and release excess carbon, hence its categorization as an "overflow" metabolite [6], [7]. In order to reduce loss of acetyl-CoA to acetate and increase carbon flux towards PHB production, we performed and investigated the effects of deleting the genes encoding for *ackA* and *pta* (Fig. S1). The primary protocol to perform these gene deletions involves a recombineering approach that combines the phage-derived lambda red system with CRISPR-Cas9 as the expression system. A fluorometric acetyl-CoA assay was used to measure the intracellular acetyl-CoA concentrations.

The TCA cycle is another major component of the central *E. coli* metabolism that consumes acetyl-CoA. As one of the mechanisms involved in aerobic respiration, it is responsible for producing one ATP, two CO_2, three NADH, one $FADH_2$, and three H^+ per molecule of acetyl-CoA consumed [8]. The loss of carbon through CO_2 in this process is especially undesirable for the purpose of reserving acetyl-CoA for PHB production as carbon flux through respiration is irreversible. In addition to producing these immediate cofactors and metabolites of respiration, the TCA cycle provides an intermediary pathway for the synthesis of important carbohydrates and amino acids across its various enzymes. These functions render the TCA cycle essential for facilitating growth in *E. coli*, but certain components can be selectively omitted without comprising the TCA cycle. We investigate an optimal set of gene knockouts involving TCA cycle reactions *in silico* using metabolic modeling.

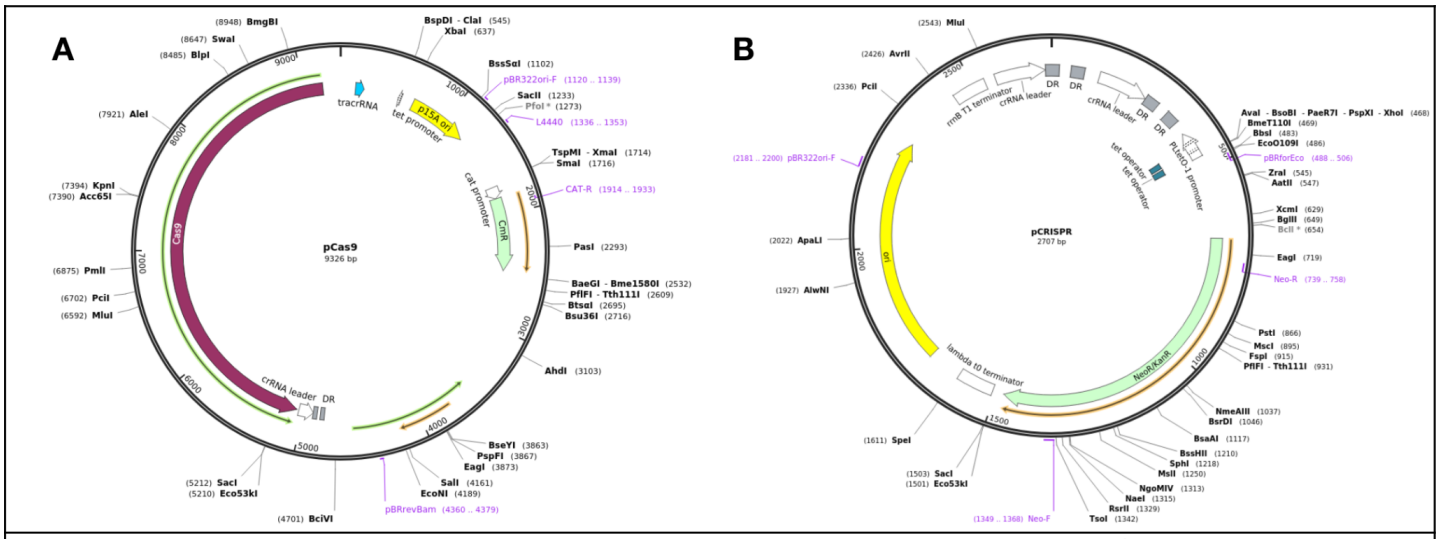

Fig. 2. pCRISPR and pCas9 Design. Visualization of the pCRISPR (A) and pCas9 (B) design created with SnapGene®.

With these three components of acetyl-CoA regulation in mind, this work seeks to provide a comprehensive solution for increasing PHB yield in our sponsor's modified *E. coli* strain to improve the mass manufacturing of microbially produced bioplastics.

Materials and Methods

Bacterial Culturing Procedure

Luira-Bertani (LB) plates were streaked with *E. coli* K-12 MG1655 by using a sterile loop and then incubated at 37 °C. The reagents and volumes for 500 mL of the LB solution consisted of: tryptone (5 g), NaCl (5 g), yeast extract (2.5 g), and milliQ water (500 mL). After the incubation period, the starter cultures were prepared with 2 mL of LB media and incubated at 37 °C for 6 hours at 200 rpm.

Coupling CRISPR/Cas9 with Lambda Red

Design and Cloning of CRISPR/ Cas9 Plasmid

Sequences ascribed to the selected knockouts were provided by the NIH Gene Library, a large collection of DNA fragments from model organism databases. An overview of plasmid construction (further detailed in the following sections) consists of digesting the chosen DNA sequence with restriction enzymes in preparation for ligating the resultant DNA fragments. The sgRNA target strand was cloned into the CRISPR plasmid in order to guide the Cas9 nuclease to the target locus (Fig. 2). The Cas9 plasmid was constructed carrying lambda red genes which encode for phage-derived proteins necessary for enabling recombination of DNA fragments (Fig. 2).

Vector Digest

In order to perform vector digestion, 1-2 µg of pCRISPR and pCas9 with BsaI (NEB) was digested. This includes a selective amount of pCRISPR or pCAS9, 1 µl of BsaI (NEB), 5 µl of 10X NEB buffer, and a selective amount of ddH20. The total volume reached 50 µL and the gel was used to purify the plasmids.

Annealing of Oligos

Oligonucleotides were ordered with the 5' end already phosphorylated and used for the annealing in order to create double-stranded DNA (dsDNA). Then, 2.5 µL of 1 M NaCl was added to the phosphorylated oligo pairs. The 5' end of the oligonucleotides were incubated at 95 °C and then slowly cooled down to room temperature using a thermocycler. The annealed oligos were then diluted 10 times.

DNA Ligation

The procedure for an agarose gel electrophoresis was followed, and the DNA (plasmid) fragments were run on a 0.8% agarose gel. After the gel was run, it was moved to an open UV box. With a clean, sterile razor blade, the desired DNA fragments were sliced from the gel. It was important to ensure that the DNA was minimally exposed to the UV light in order to prevent dimer formation. Each fragment was then placed into separate, sterile eppendorf tubes. The agarose fragments were then melted by placing them in a 65 °C water bath for 10 minutes and held at room temperature. In a sterile eppendorf tube, 20 µL of a ligation reaction was prepared by combining: 2 µL of T4 DNA Ligase Buffer (10X), 10 µL total of agarose DNA, 7 µL of MilliQ Water, and 1 µL of T4 Ligase. The water, buffer, and vector were added first, and the ligase was added after. The reaction mixture was ligated for a total of

3 hours at room temperature, and the first insert was added at the beginning, the second insert was added after 30 minutes, and all of the following inserts were added in 15 minute increments, starting with the vector. Using 2-4 µL of the ligation reaction, the plasmids were then transformed.

Ethanol Precipitation of RNA/DNA to purify ligation reaction

0.1 volume of 3 M sodium acetate was added to 2.5-3 volume of ice cold 100% ethanol then vortexed thoroughly. Afterwards, the solution was precipitated at -20 °C for 1 hour and centrifuged at 13,000 rpm at 40 °C for 30 minutes. The pellets were then washed twice with 0.5 mL of ice cold 70% ethanol and spun at 40 °C for 10 minutes each time. The ethanol was then taken out and spun quickly for 10 seconds at the top speed in order to remove any trace amounts of ethanol. The pellets were air dried and resuspended in an appropriate volume of nuclease free water.

Preparing Electrocompetent Cells

400 mL of *E. coli* culture was grown to 0.5-0.7 to an optical density of 600 nm (OD_{600}). If the cells were already transformed with the Cas9 plasmid and were being made re-competent, the cells were cultured at 42 °C for 15 minutes in order to heat-shock induce the lambda red recombineering. The culture was then left on ice for 15-30 minutes. After that, the cells were pelleted at 4 °C for 15 minutes at 4000 *g*. The supernatant was decanted and the pellets were resuspended in 400 mL of ice-cold 10% sterile glycerol. The previous step was repeated and resuspended in 10 mL of 10% sterile glycerol. The previous step was repeated once more, and resuspended in 0.8 mL in 10% sterile glycerol. 50 µL aliquots were made of the cell suspension and worked on ice. The aliquots were then frozen in liquid nitrogen and stored at -80 °C.

Electroporations

The Recovery Medium and sterile culture tubes were readily prepared at room temperature (one tube for each transformation reaction). The electroporation cuvettes (0.1 cm gap) and microcentrifuge tubes were placed on ice (one cuvette and one microfuge tube for each transformation reaction). The cells were then removed from the -80 °C freeze and thawed completely, which took about 10-15 minutes. Once the cells were thawed, they were mixed by gently tapping them. 25 µL of the cell/DNA mixture was pipetted into a chilled electroporation curbette, ensuring that no bubbles were introduced. The cell/DNA mixture was then tapped down to the bottom of the cuvette. Within 10 seconds of the pulse, 1 mL of the Recovery Medium was added to the cuvette and pipetted up and down three times in order to resuspend the cells. The cells and Recovery Medium were transferred into a culture tube and placed in a shaking incubator at 250 rpm for 1 hour at 37 °C. Up to 100 µL of the transformed cells were spread on LB agar plates containing the appropriate antibiotic. The plates were incubated overnight at 37 °C. The transformed clones could then be further grown in Terrific Broth (TB) or in another rich culture medium.

DNA Extraction

The procedure for DNA extraction was followed by first transferring 1-1.5 mL *E. coli* culture to 1.5 mL microcentrifuge tube and centrifuge at 10,000 rpm (8,000 - 10,000 x *g*) for 30 seconds. The supernatant was removed and discarded. Then, 250 µL Lysis Buffer was added to the mixture and mixed gently by inverting the tube 4-6 times in order to avoid contamination by genomic DNA. Following that, 350 µL of Neutralization Buffer was added and mixed gently by inverting the tube 4-6 times. The solution should become cloudy and no local precipitate should be visible. The mixture was then centrifuged at 13,000 rpm (> 14,000 x *g*) for 10 minutes until a compact white pellet forms. The supernatants were then transferred to the Spin column and centrifuge for 30-60 seconds at 6,000 x *g*. All the flow-though were discarded. Then, 650 µL Wash Buffer was added to the Spin column and centrifuged for 30-60 seconds at 12,000 x *g*. The flow-through was discarded and this step was repeated once. This Spin column was centrifuged for an additional 1 minute at 12,000 x *g* in order to remove residual and then transferred the Spin column to a sterile 1.5 mL microcentrifuge tube. Then, 50 µL Elution Buffer (ddH2O or TE Buffer) was added to the Spin column and allowed the column to stand for 1 minute at room temperature. Then, the Spin column was centrifuged again at 12,000 x *g* for 1 minute. The buffer in the microcentrifuge tube contains the plasmid. The DNA was stored at -20 °C.

Restriction Enzyme Digest (Generic)

In order to make the 50 µL Reaction the following were added together: 1 µg of DNA, 5 µL of respective NEB buffer (10X), 1 µL of enzyme 1, 1 µL of enzyme 2, and the remaining was filled with MilliQ Water. In the reaction tube, water, buffer, DNA, and enzymes were mixed in the order as listed. The reaction mixture was incubated at 37 °C for 30 minutes then heat killed at 80 °C for 20 minutes.

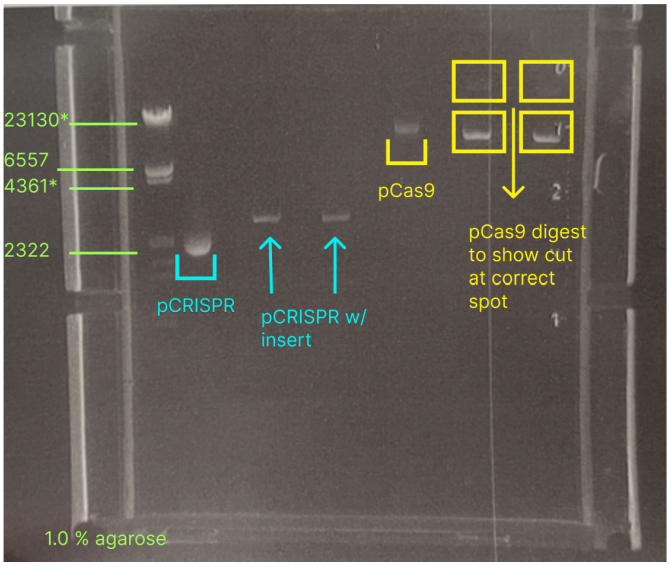

Fig. 3. Restriction Enzyme Digest. Digest was used to confirm that the pCas9 and CRISPR plasmids have been constructed correctly and successfully. The bands line up to the corresponding kDa values.

A restriction enzyme digest was performed to confirm the successful construction of the pCas9 and pCRISPR plasmids (Fig. 3). The ones labeled with CRISPR show that the inserted plasmid is larger than the pCRISPR without the insert. The pCas9 plasmid is digested with one restriction enzyme that is unique to the insert (BamHI) and one that makes a single cut in the backbone, so two bands would not be seen unless the inserts were present.

Growth Curve Measurements

In order to produce the growth curves, 50 mL cultures were inoculated with 2 mL starter cultures for 12 hours. The measurements for OD_{600} were taken after the first 30 minutes of incubation and then every 60 minutes following that up until 585 minutes. Growth curves were described using the Power Type Growth model–an empirical sigmoidal growth model. Microbial growth with a single inflection point is commonly described using sigmoidal functions [9].

$$y(t) = y_0 + \frac{At^n}{b+t^n} \quad [1]$$

Equation (1) displays the Power Type Growth, where the time in minutes (t) is correlated to OD_{600} in nm ($y(t)$). The variables A, b, and n are empirical parameters, while y_0 is the initial OD_{600} of the sample group. MATLAB's curve-fitting tool was used to determine the empirical parameters for each sample group. All samples began at an initial OD_{600} of zero (y_0=0).

$$t_{ifx} = \sqrt[n]{\frac{b(n-1)}{n+1}} \quad [2]$$

$$y_{ifx} = \frac{A(n-1)}{2n} \quad [3]$$

The growth curves can be further characterized by determining the inflection times (t_{ifx}) and responses (y_{ifx}) by substituting the empirical values into equation (2) to allow for comparison of the rate of growth between sample groups (e.g., a smaller inflection time indicates quicker growth) [9].

Acetyl-CoA Absorbance Assay

Acetyl-CoA concentrations were determined for each sample group (i.e., control, ΔackA, and Δpta) using an acetyl-CoA assay kit from abcam (ab87546). Acetyl-CoA was measured indirectly by measuring nicotinamide adenine dinucleotide (NADH), which is the product formed after reacting it with free coenzyme A (CoA) that was converted from the acetyl-CoA. Standard curve calibrations were determined using fluorometric readings from samples of known acetyl-CoA concentrations for each assay performed. MATLAB's curve-fitting tool was used to determine the standard calibration curves for acetyl-CoA.

$$y = ax^2 + bx + c \quad [4]$$

$$y = mx + B \quad [5]$$

Equation (4) is a typical acetyl-CoA 0.1 nmol standard calibration curve, while Equation (5) is a typical acetyl-CoA 0-100 pmol standard calibration curve. The relationship between absorbance (y) and the acetyl-CoA concentration (x) is a second-degree polynomial and a linear function for a 0.1 nmol and 0-100 pmol typical acetyl-CoA standard calibration curve, respectively, where a, b, c, m, and B are the coefficients and/or constants determined from MATLAB's curve-fitting tool. The standard curves were used to determine the acetyl-CoA concentrations of the control and experimental samples by using their collected absorbance values. Since the acetyl-CoA concentrations of the samples were visible in the assay in the 0.1 nmol range and exceed that of the 0-100 pmol range, equation (4) was used as the standard calibration curve.

Fluorometric Readings

Fluorometric readings were determined using FilterMax™ F5 Multi-Mode Microplate Reader with 535 nm excitation filter (Ex) and 595 nm emission filter (Em). The emission filter for the microplate reader on the given protocol suggested using 587 nm. However, due to limited options on the filters, the 595 nm emission filter was used instead. An opaque 96-well plate was used to minimize background fluorescence and crosstalk [10].

Determination of Acetyl-CoA Concentrations

Five independent assays were performed for each sample group (n=5) with their average acetyl-CoA concentration determined by averaging five trials of their respective determined acetyl-CoA concentrations generated by inputting their absorbance values into their associated standard curve. Each sample is equivalent in the amount of bacteria (i.e., 10 µL of the cultured bacteria) and can thus be averaged as one single value. To allow for comparison between the sample groups, acetyl-CoA concentrations were normalized by dividing the cell culture wet weight to their respective independent sample to provide normalized acetyl-CoA concentrations (µM/mg). The cell culture wet weight was determined by subtracting the mass of an empty microcentrifuge tube from its respective tube with the wet cell culture pellet. A digital analytical balance was used to determine these masses. Uncertainty was determined by taking the standard deviation of the normalized acetyl-CoA concentrations of each sample group.

Statistical Analysis of Acetyl-CoA Concentrations

A one-way analysis of variance (ANOVA) followed by a Tukey test (i.e., a multiple comparisons test) was used to determine if and which sample groups exhibited any significant difference between their means (i.e., control, ΔackA, and Δpta). Significant results were determined at a 95 percent confidence level ($p<0.05$).

Genome-Scale Metabolic Model (GEM)

Plasmid Inclusion and Model Verification

A pre-existing GEM for *E. coli* K-12 MG1655, iML1515, was selected from the Biochemical, Genetic, and Genomic (BiGG) database for modification to accommodate the inclusion of the *pha* and *sty* plasmids and their respective constraints. The COnstraint-Based Reconstruction and Analysis (COBRA) Toolbox and COBRApy were used to modify, and analyze the existing iML1515 model to include the reactions and metabolites conferred by the *sty* and *pha* plasmids within our modified bacteria. In addition to these reactions, transport, exchange, and demand reactions were added to allow styrene and PHB to enter and exit the system (Table S2). These additions to the model were visualized with Escher, a mapping tool for GEMs [11]. Flux balance analysis (FBA) was used to verify that the modified GEM maintains steady state conditions, where the net flow of metabolites in and out of the system is zero. Influx rates for all metabolites defined in the growth medium were constrained to zero, and the objective was set to maximize biomass production. The cell was unable to produce biomass, indicating a lack of any mass generating reactions in the model and proper mass conservation. Additional optimizations were performed after removing the constraint on a single input metabolite such as styrene, oxygen, or phosphate one at a time. In all cases, the model was unable to generate any biomass regardless of the metabolite that was added to the system, indicating validity of the model.

Robustness Analysis

Robustness analysis was performed on the model using the robustness analysis function from COBRA Toolbox (Fig. S3). The carbon source uptake rates associated with the greatest PHB production rates were selected as constraints for FBA optimizations to determine uptake and secretion rates for the remaining metabolites in the model. Molar ratios between input and output metabolites were then used to determine stoichiometric yields of PHB and CO_2.

OptKnock Algorithm

Growth-coupled PHB production was explored with OptKnock, an algorithm that selectively knocks out sets of genes to alter metabolism and couple the flux of a chosen reaction to the objective function, making one dependent on the other (Fig. S4). The maximum number of gene deletions in the solution was set to three to reflect a realistic number of concurrent knockouts. Production envelope data were predicted using COBRA Toolbox for all gene knockout sets tested to visualize the extent of function-coupled PHB production. Figures were generated in R using ggplot2 using results from MATLAB.

Results

In silico metabolic model analysis of PHB production on styrene and glucose media

Robustness Analysis

Robustness analysis performed on the updated metabolic model provided PHB yield rate as a function of carbon uptake rate. PHB production was characterized for styrene M9 media, and carbon uptake rates were constrained from 0 to -13 mmol/gDWh. PHB yield reached a peak of 9.239 mmol/gDWh at -6.159 mmol/gDWh styrene uptake. Following this maximum, PHB yields gradually decreased to zero with increasing styrene. This indicates that higher concentrations of styrene in the growth media is detrimental to PHB production, which may be partly due to a limiting reactant within the metabolism. Previous work has shown that oxygen was the limiting reactant due to the high amounts

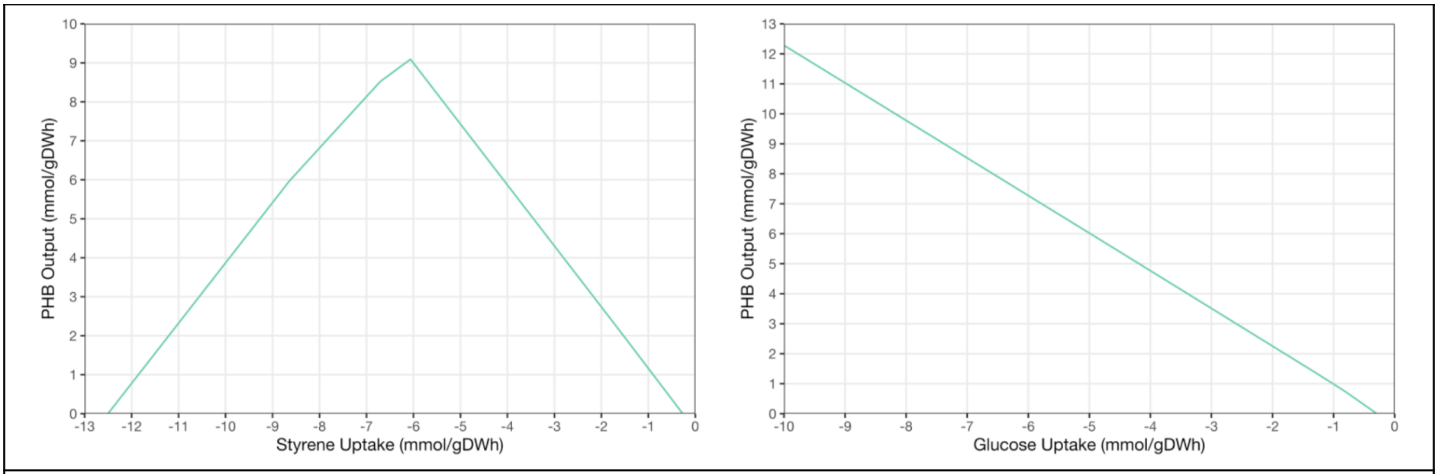

Fig. 4. Robustness analysis results indicating PHB yield rates as a function of carbon uptake rate. For growth on styrene, the model was constrained from 0 to -13 mmol/gDWh styrene uptake and M9 minimal media conditions. For glucose, the model was constrained to 0 to -10 mmol/gDWh glucose uptake and M9 minimal media conditions. Y-axes indicate flux towards the target reaction, and x-axes indicate flux towards PHB production. Positive fluxes indicate flow through reactions in the forward direction, while negative fluxes indicate flow in the negative direction. Exchange reactions, which are used here to represent styrene uptake and PHB output, indicate secretion of metabolites rather than uptake by default.

of oxygen required to metabolize styrene [12]. These patterns are not seen with growth on glucose, which showed a steady increase in PHB production from 0 to -10 mmol/gDWh glucose uptake. PHB yield rate reached a peak of 12.28 mmol/gDWh at a maximum glucose uptake rate of -10 mmol/gDWh. This indicates that cells grown on glucose are theoretically able to use all the glucose they consume for PHB production (Fig. 4).

Stoichiometric Yields

The peak PHB production rate associated with styrene (9.239 mmol/gDWh) was used to obtain optimal stoichiometric yields of PHB. Simple division of the styrene uptake rate (6.159 mmol/gDWh) at its peak PHB yield rate (9.239 mmol/gDWh) provided an approximate molar ratio of 1:1.5 for styrene to PHB. Given that there are four carbons in one molecule of PHB and eight carbons in one molecule of styrene, there is an observed loss of carbon when styrene is converted into PHB. The extra carbon is converted into carbon dioxide (CO_2), which is produced at about 12.28 mmol/gDWh at 6.159 mmol/gDWh styrene uptake. This is approximately equivalent to a molar ratio of 2:1 for CO_2 to styrene. This produces a total molar ratio of 1:1.5:2 for styrene uptake to PHB to CO_2 yield.

In comparison to glucose, dividing the glucose uptake rate (10 mmol/gDWh) at its peak PHB yield rate (12.28 mmol/gDWh) provided an approximate molar ratio of 1:1.2 for glucose to PHB. Although this is a lower molar ratio than seen with styrene, one molecule of glucose contains six carbons, demonstrating a reduced loss of carbon. At -10 mmol/gDWh glucose uptake, the CO_2 yield rate is 10.87 mmol/gDWh, providing a net approximate carbon molar ratio of 1:1.2:1 for glucose uptake to PHB to CO_2 yield. In contrast to styrene, less carbon is lost as CO_2 in PHB production using glucose substrate.

In vivo effects of ΔackA and Δpta on cell growth and acetyl-CoA yield

Growth Curves

The control had the most rapid and steady growth rate out of the three sample groups (i.e., control, ΔackA and Δpta), exhibiting an inflection point–the point of most rapid growth–at 168 minutes (Fig. 5). This is 21.9 and 22.6 percent faster than the inflection time points for ΔackA (215 minutes) and Δpta (217 minutes), respectively. Furthermore, the OD_{600} (i.e., the model's response) at these inflection points for the control was 1.5 nm, which is greater than ΔackA (1.3 nm) and Δpta (1.4 nm). On the other hand, this reveals that ΔackA had the slowest growth rate and max out of all sample groups. Despite the revelation that the knockouts (ΔackA and Δpta) did not exhibit a faster growth rate or a greater max growth in comparison to the control, the ability to characterize and fit the growth curves to typical ones observed in bacteria demonstrate that the knockouts were not substantially detrimental to cell growth.

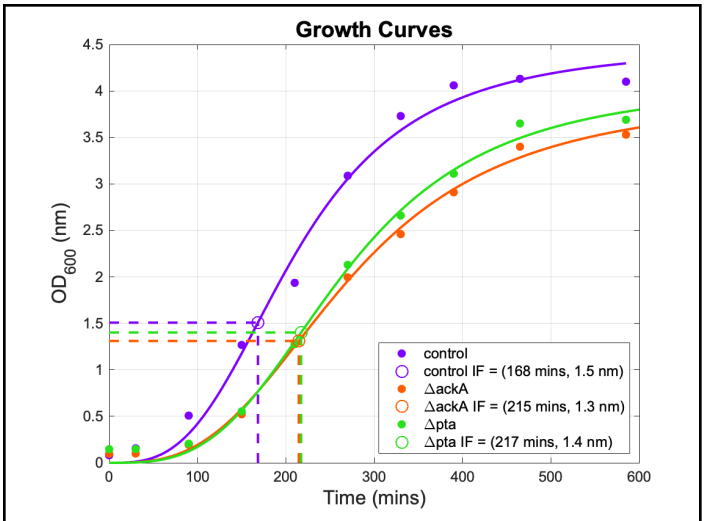

Fig. 5. Growth Curves of Sample Groups. Growth curves of control, Δpta, and ΔackA were characterized using a Power Type Growth over a 12 hour period. Inflection points (IF) are circled on the growth curve and directed by dotted lines to display the fastest rate of growth for each sample group. The values for each IF are stated in the legend. The control demonstrates the fastest and most steady growth rate out of the three experimental groups. The ackA knockout demonstrates the slowest growth rate compared with the other two groups.

Acetyl-CoA Concentrations

Acetyl-CoA concentrations were quantified fluorometrically and normalized using their cell culture wet weight resulting in 0.041±0.006, 0.027±0.007, and 0.039±0.007 µM/mg for control, ΔackA, and Δpta, respectively (Fig. 6). ΔackA was significantly lower than the other samples, exhibiting a fold decrease of 1.5 between control and 1.4 between Δpta (p<0.05). On the other hand, Δpta exhibited no significant difference between control samples, exhibiting a fold decrease of 1.1.

Proposal of succinyl-CoA synthetase deletion with *in silico* metabolic model optimization

OptKnock Algorithm

Previous studies have indicated that no set of gene knockouts can induce growth-coupled PHB production in *E. coli* using styrene as the primary carbon source [12]. Results from the OptKnock algorithm run on our model confirm these findings, as it provided no candidate reaction knockouts. However, running the algorithm again using glucose as the carbon source and ATP maintenance as the objective function did provide an ATP-coupling reaction knockout set that includes the isocitrate dehydrogenase reaction (ICDHyr) and acetate exchange reactions from the model. ICDHyr is an enzyme in the TCA cycle that catalyzes the conversion of isocitrate to α-ketoglutarate, which is used downstream to produce essential amino acids glutamate and glutamine. While this deletion prevents the cell from producing any biomass and is lethal to the cell, other reaction knockouts were tested in model to determine if a less vital reaction could be knocked out instead. Exploring other knockout sets involving acetate exchange reactions and other TCA cycle enzymes provided a viable set that replaces ICDHyr deletion with

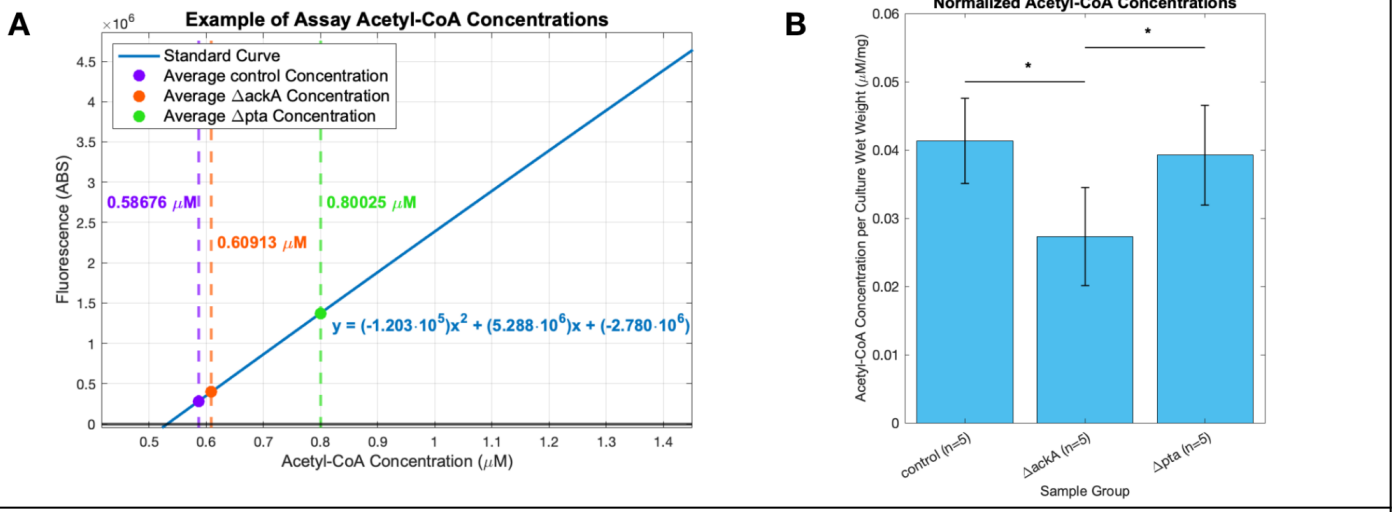

Fig. 6. Sample *E. coli* Acetyl-CoA Concentrations. (A) A single acetyl-CoA assay includes five trials for each sample group (i.e., control, ΔackA, and Δpta). An example of the determination of the acetyl-CoA concentrations from the five absorbance values for each sample using their respective standard curve from their assay is shown. The standard curve was fitted as a second-degree polynomial using MATLAB's curve-fitting tool. The acetyl-CoA concentrations are not yet normalized for comparison. (B) The average acetyl-CoA concentrations from five assays (n=5) were normalized by dividing them by the cell culture wet weight and averaged to produce a single normalized acetyl-CoA concentration value in micromolar per milligram (µM/mg). These values are displayed on the graph as 0.041±0.006, 0.027±0.007, and 0.039±0.007 µM/mg of acetyl-CoA per wet cell culture weight for control, ΔackA, and Δpta, respectively.

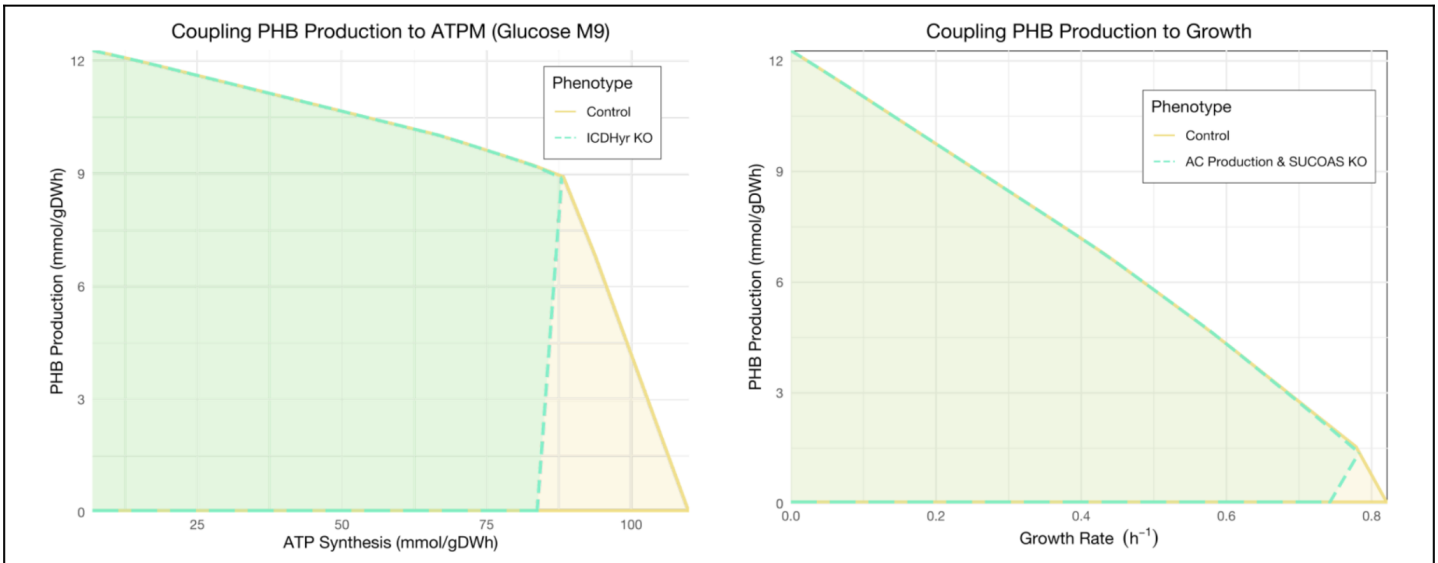

Fig. 7. Production Envelopes Comparing Simulated Gene Modifications to Control on Glucose M9 Media. 'ICDHyr' refers to knockout of isocitrate dehydrogenase. 'AC Production' refers to deletion of acetate exchange reactions, which completely prevents acetate from being secreted from the system. 'SUCOAS' refers to knockout of succinyl-CoA synthetase. Model was constrained to 10 mmol/gDWh glucose uptake and M9 minimal media conditions. Y-axes indicate flux towards the target reaction, and x-axes indicate flux towards ATP synthesis or biomass production (growth).

knockout of succinyl-CoA synthetase (SUCOAS), a downstream TCA cycle reaction. While ICDHyr catalyzes a vital reaction, SUCOAS is responsible for the aerobic portion of the TCA cycle and is therefore not lethal as respiration can be taken up by other components of the metabolism. PHB production envelopes for growth on glucose with and without these reaction knockouts were simulated to visualize the extent of growth-coupling induced by modifications (Fig. 7). With knockout of SUCOAS and acetate exchange reactions, PHB production continued to be coupled with ATP synthesis as seen with ICDHyr, but also allowed the cell to continue producing biomass. Furthermore, this knockout set constrains the production of biomass enough to weakly couple PHB production to growth. The highest growth rate in these cells requires a PHB production rate of 1.379 mmol/gDWh, compared to 0 mmol/gDWh in the control model. This shows that with SUCOAS knockout and deletion of acetate exchange reactions, the constrained metabolism requires the cell to produce PHB at a low rate when growing rapidly.

For laboratory applications, the genes and pathways associated with these reactions were identified within the model as follows. The SUCOAS reaction corresponds to genes sucC and sucD, whereas knockout of acetate exchange reactions can be approximated by deleting genes encoding for acetate production pathways in the cell. These include genes that encode for ackA-pta, aldehyde dehydrogenase, citrate lyase, and acetyl-CoA:hexanoate-CoA transferase.

Discussion

For the overall goal of increasing intracellular acetyl-CoA concentrations in our bacteria, we focused on three major components of the *E. coli* metabolism: glucose uptake through glycolysis, acetate production through the ackA-pta pathway, and the TCA cycle. While our selection of glucose as our feedstock trades off the recyclability offered by styrene, we anticipate greater yields of PHB by avoiding any metabolic inefficiencies caused by PHB production on styrene.

In choosing an optimal carbon source for PHB production, both the robustness analysis results and stoichiometric yields calculated from the model indicate that glucose is the superior carbon feedstock. In contrast to styrene substrate, the metabolic capacity of the cell does not reach a maximum limit in its carbon uptake for PHB production. Furthermore, simulated optimal stoichiometric yields of PHB indicate that less carbon is lost as CO_2 with glucose substrate. While a feedstock combining both styrene and glucose to compromise between recyclability and metabolic efficiency could be explored, such a growth medium is not likely to be effective due to a phenomenon known as carbon catabolite repression (CCR) [13].

CCR is a global regulatory mechanism in bacteria that selectively inhibits the expression and activities of functions associated with the use of secondary carbon sources when another preferred carbon source is present

[14]. CCR is believed to be an important strategy for bacterial growth in natural environments as it prioritizes the consumption of simpler sugars over more complex ones in order to reduce the greater energy expenditure associated with catabolism of more complex sugars [13]. Therefore, the preference for the bacteria to utilize glucose over styrene can be explained by the greater complexity of styrene's chemical structure. The chemical structure of styrene consists of an aromatic hydrocarbon (exhibiting multiple double carbon bonds) with an attached alkene side group, whereas glucose's chemical structure consists of a simpler aldose ring (exhibiting only single carbon bonds)[15]. The higher bond dissociation energy associated with styrene causes this molecule to be less preferred as a carbon source. In addition, oxygen was found to be a limiting reactant in the robustness analysis of styrene which may be attributed to the reliance on oxygen as a part of styrene's degradation. Oxygen is required both for side chain oxygenation and direct ring cleavage of styrene, meaning that styrene utilization is contingent on the availability of oxygen [15].

With knockout of ackA-pta, we did not see expected increases in acetyl-CoA concentrations, but we speculate this may be caused due to funneling of additional acetyl-CoA into PHB production. Acetyl-CoA is one of the most highly regulated metabolites within *E. coli* as it represents a key node in the intersection of several metabolic pathways. In the context of the ackA-pta pathway, acetyl-CoA concentration is regulated based on the concentration of acetyl phosphate. The pta enzyme synthesizes acetyl phosphate and CoA from acetyl-CoA and available phosphate groups, whereas the ackA enzyme generates ATP from the acetyl phosphate and ADP while simultaneously producing acetate. Thus, the steady-state concentration of acetyl phosphate is dependent on the rate of its formation, as catalyzed by pta, and its rate of degradation, as catalyzed by ackA. This information may elucidate the reason for the observed decrease in acetyl-CoA concentration in the ackA knockout compared to the observed indifference in acetyl-CoA concentration in the pta knockout. Acetyl-phosphate is also known to be related to global regulation because of its ability to activate response regulators of two-compartment systems and its control over the metabolic fluxes [16].

In addition, an influx of excess acetate has been observed to be detrimental to the cell's maximum growth on glucose by perturbing fluxes in central metabolism (i.e., the perturbation of acetate metabolism) [17]. The acetate pathway is an important pathway for ATP production, since the ackA-pta pathway is the predominant generator for acetate [16]. ATP production generated from the ackA-Pta pathway is essential for cell growth, since the ackA enzyme converts acetyl phosphate into acetate and subsequently ATP. Without the ackA enzyme to convert acetyl phosphate into acetate and ATP, the cell loses an energy source fueling its metabolism thus hindering cell growth.

The growth reduction of the ackA deletion may also be due to the production of acetyl phosphate that leads to increased protein acetylation, as it is known to be an acetyl donor [16]. The hydrolysis of acetyl-phosphate in this intermediate pathway is not coupled to ATP generation, which may lead to low ATP content and low growth rate in the ackA knockout. Additionally, acetyl phosphate is also involved in the acetylation of enzymes and regulatory proteins that have broad physiological consequences [17].

As for inducing growth coupling in our cells, the production envelopes demonstrate a notable change in the metabolism of our bacteria. In control cells simulated to grow in optimal conditions, growth does not require PHB production. With the proposed deletion of SUCOAS in the TCA cycle and acetate production pathways, cells must achieve a PHB yield rate of 1.379 mmol/gDWh in order for the cells to reach their maximum growth rate. This guarantees a baseline level of PHB production when cells are actively growing.

To explain the extent of growth coupling evident in our model, deletion of the acetate production pathways prevents the cell from funneling excess acetyl-CoA into acetate and opens up possibilities for carbon overflow through other metabolites such as ethanol, aldehyde, or PHB. Additionally, removal of acetate production pathways increases the availability of acetyl-CoA for use in other pathways, including for PHB production. Combining this modification with knockout of SUCOAS, which activates the glyoxylate shunt and prevents the loss of carbon to CO_2 by the bypassing of the aerobic portion of the TCA cycle, helps reserve additional carbon flux towards PHB (Fig. S5). Removal of these pathways also alters the balance of cofactors, such as CoA, within the metabolism. CoA is a cofactor produced by both ackA and SUCOAS, and removal of these reactions reduces the net production of CoA within the metabolism. The PHB production pathway involves two reactions that produce CoA as byproducts, and so we hypothesize that these knockouts encourage the cell to use the PHB production pathway to compensate for lower CoA in the cell. While PHB itself is not used in the *E. coli* metabolism, the pathway associated with its production is more essential with these reaction knockouts.

Limitations

Because the concentrations of other cofactors involved in the ackA-pta pathway (i.e., acetate and acetyl-phosphate) were not measured, the impact of the knockouts on the cell's metabolism cannot be fully characterized. This limits the ability to verify the cause in the reduction of acetyl-CoA. In addition, the absence of gas chromatography data from the knockout groups hinders our ability to make a definitive conclusion of ackA-pta gene deletion on PHB yield.

The lack of experimental data of our modeling results on the *in vivo* relationship between PHB production on glucose substrate cannot validate our model's expectation of glucose being a superior feedstock to styrene. Furthermore, the lack of *in vivo* validation of the model's prediction of growth-coupling for PHB production by knocking out SUCOAS and acetate production cannot confirm the accuracy of our model to predict optimized knockouts. Although sequencing of the cells with the knockouts was initiated to provide validation of successful gene knockouts, timing conflicts have prevented the inclusion of this data.

Future Directions

In vivo application of our model's predicted knockouts would not only aid in investigating other potential pathways to help increase intracellular acetyl-CoA concentrations, but confirm the accuracy of our metabolic model. Further assays should be performed to measure the knockouts' effect on the concentration of acetate, acetyl-phosphate, and other associated cofactors as well as effects on the cell's metabolism. Moreover, the impact of our hypothesized gene deletions on increasing PHB yield will be confirmed through gas chromatography.

End Matter

Author Contributions and Notes

Hannah Towler was the technical trainer and supervisor. Julia Yao performed data analysis of fluorometric readings. Sang-Hoon Park performed GEM editing and synthesized modeling results. Xin Chen, Tammy Tran, and Thomas Nguyen assisted in acetyl-CoA assay production and general research.

Acknowledgments

This work was funded in part by Transfoam LLC, located in Charlottesville, Virginia and the University of Virginia (UVA).

We thank our advisors in Transfoam–Simonne Guenette (Co-Founder & CTO), Kobe Rogers (Co-Founder & COO), and Alec Brewer (Co-Founder & CEO)–and our co-advisors at UVA–Mark Kester (Department of Pharmacology, Biomedical Engineering, Molecular Physiology and Biophysics) and Keith Kozminski (Doctor of Philosophy, Departments of Biology and Cell Biology)–for critically reading and commenting the manuscript and providing aid and guidance to our research. We would also like to thank Dr. Timothy Allen, Dr. Shannon Barker, Capstone TAs, and Dr. Glynis Kolling for the additional help with obtaining and sourcing laboratory materials.

Fluorometric readings were generated using FilterMax™ F5 Multi-Mode Microplate Reader located in University of Virginia Integrative Design & Experimental Analysis (IDEAS) Laboratory. CRISPR/Cas9 was performed in the University of Virginia Physical Life Science Laboratory.

References

[1] H. Ritchie and M. Roser, "Plastic Pollution," *Our World Data*, Sep. 2018, Accessed: Apr. 23, 2022. [Online]. Available: https://ourworldindata.org/plastic-pollution

[2] G. Atiwesh, A. Mikhael, C. C. Parrish, J. Banoub, and T.-A. T. Le, "Environmental impact of bioplastic use: A review," *Heliyon*, vol. 7, no. 9, p. e07918, Sep. 2021, doi: 10.1016/j.heliyon.2021.e07918.

[3] C. R. Hankermeyer and R. S. Tjeerdema, "Polyhydroxybutyrate: plastic made and degraded by microorganisms," *Rev. Environ. Contam. Toxicol.*, vol. 159, pp. 1–24, 1999, doi: 10.1007/978-1-4612-1496-0_1.

[4] A. Getachew and F. Woldesenbet, "Production of biodegradable plastic by polyhydroxybutyrate (PHB) accumulating bacteria using low cost agricultural waste material," *BMC Res. Notes*, vol. 9, p. 509, Dec. 2016, doi: 10.1186/s13104-016-2321-y.

[5] B. McAdam, M. Brennan Fournet, P. McDonald, and M. Mojicevic, "Production of Polyhydroxybutyrate (PHB) and Factors Impacting Its Chemical and Mechanical Characteristics," *Polymers*, vol. 12, no. 12, p. 2908, Dec. 2020, doi: 10.3390/polym12122908.

[6] "Control and regulation of acetate overflow in Escherichia coli | eLife." https://elifesciences.org/articles/63661 (accessed May 04, 2022).

[7] N. S. Parimi, I. A. Durie, X. Wu, A. M. M. Niyas, and M. A. Eiteman, "Eliminating acetate formation

improves citramalate production by metabolically engineered Escherichia coli," *Microb. Cell Factories*, vol. 16, p. 114, Jun. 2017, doi: 10.1186/s12934-017-0729-2.

[8] "The Tricarboxylic Acid Cycle at the Crossroad Between Cancer and Immunity | Antioxidants & Redox Signaling." https://www.liebertpub.com/doi/10.1089/ars.2019.7974 (accessed May 04, 2022).

[9] D. A. Longhi, F. Dalcanton, G. M. F. de Aragão, B. A. M. Carciofi, and J. B. Laurindo, "Microbial growth models: A general mathematical approach to obtain μ_{max} and λ parameters from sigmoidal empirical primary models," *Braz. J. Chem. Eng.*, vol. 34, pp. 369–375, Jun. 2017, doi: 10.1590/0104-6632.20170342s20150533.

[10] "Which Plates Should I Choose for Fluorescence and Luminescence Measurements?" https://www.promega.com/resources/pubhub/which-plates-to-choose-for-fluorescence-and-luminescence-measurements/ (accessed May 03, 2022).

[11] Z. A. King, A. Dräger, A. Ebrahim, N. Sonnenschein, N. E. Lewis, and B. O. Palsson, "Escher: A Web Application for Building, Sharing, and Embedding Data-Rich Visualizations of Biological Pathways," *PLOS Comput. Biol.*, vol. 11, no. 8, p. e1004321, Aug. 2015, doi: 10.1371/journal.pcbi.1004321.

[12] "Team:Virginia/project-description - 2019.igem.org." https://2019.igem.org/Team:Virginia/project-description (accessed Nov. 16, 2021).

[13] A. Bren, J. O. Park, B. D. Towbin, E. Dekel, J. D. Rabinowitz, and U. Alon, "Glucose becomes one of the worst carbon sources for E.coli on poor nitrogen sources due to suboptimal levels of cAMP," *Sci. Rep.*, vol. 6, p. 24834, Apr. 2016, doi: 10.1038/srep24834.

[14] B. Görke and J. Stülke, "Carbon catabolite repression in bacteria: many ways to make the most out of nutrients," *Nat. Rev. Microbiol.*, vol. 6, no. 8, Art. no. 8, Aug. 2008, doi: 10.1038/nrmicro1932.

[15] M. Oelschlägel, J. Zimmerling, and D. Tischler, "A Review: The Styrene Metabolizing Cascade of Side-Chain Oxygenation as Biotechnological Basis to Gain Various Valuable Compounds," *Front. Microbiol.*, vol. 9, 2018, Accessed: May 04, 2022. [Online]. Available: https://www.frontiersin.org/article/10.3389/fmicb.2018.00490

[16] A. Schütze, D. Benndorf, S. Püttker, F. Kohrs, and K. Bettenbrock, "The Impact of ackA, pta, and ackA-pta Mutations on Growth, Gene Expression and Protein Acetylation in Escherichia coli K-12," *Front. Microbiol.*, vol. 11, p. 233, 2020, doi: 10.3389/fmicb.2020.00233.

[17] S. Pinhal, D. Ropers, J. Geiselmann, and H. de Jong, "Acetate Metabolism and the Inhibition of Bacterial Growth by Acetate," *J. Bacteriol.*, vol. 201, no. 13, Jul. 2019, doi: 10.1128/JB.00147-19.

Supplemental Material

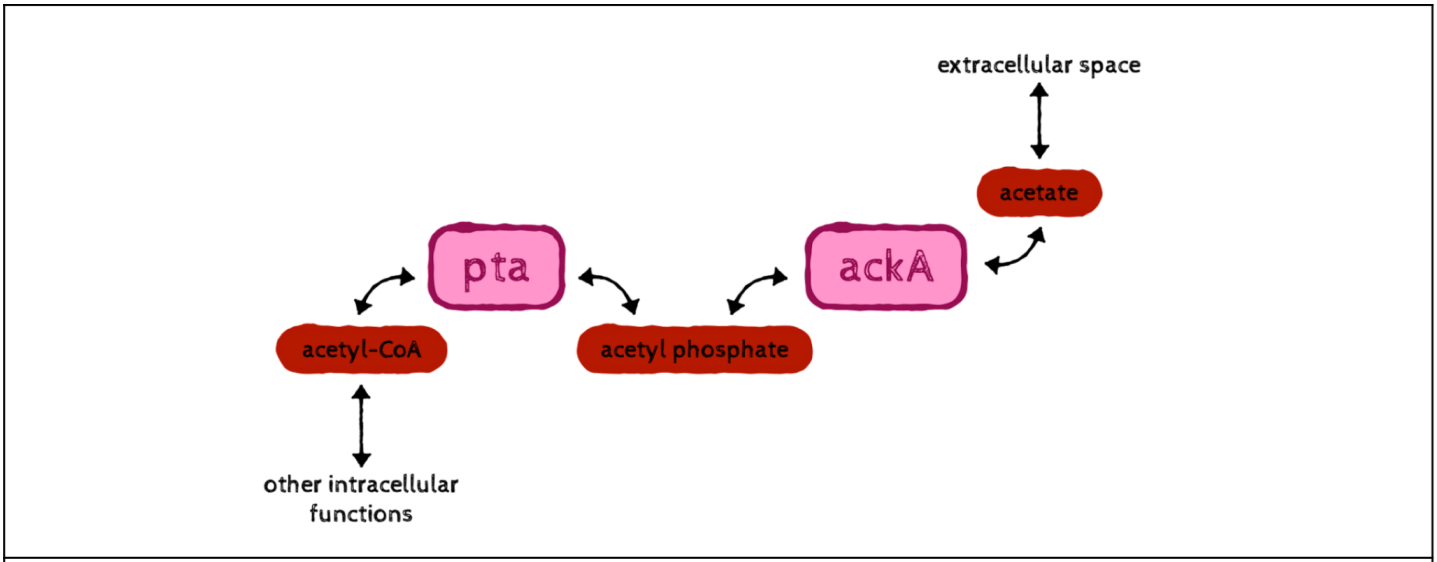

Supplemental Fig. 1. Illustration of ackA-pta Pathway. The ackA-pta pathway consists of two genes: acetyl-CoA kinase (ackA), and phosphate acetyltransferase (pta). The ackA gene is downstream of the pathway and responsible for converting acetyl phosphate into acetate and vice versa. The acetyl phosphate can then be converted into acetyl-CoA, the precursor metabolite for PHB production, through the pta gene.

Supplemental Table 2. List of Reactions Added to Model iML1515.

Gene	Reaction Name	Reaction Type	Reaction Equation
–	–	Exchange	phleth_e ⇌
–	Porin	Transport	phleth_e ⇌ phleth_p
styE	Styrene Transporter	Transport	atp_c + h2o_c + phleth_p ⇌ adp_c + h_c + phleth_c + pi_c
styAB	Styrene Monooxygenase	Metabolic	fadh2_c + o2_c + phleth_c ⇌ fad_c + h2o_c + h_c + phloxi__s2_c
styC	Styrene Oxide Isomerase	Metabolic	phloxi__s2_c ⇌ pacald_c
phaA	Acetyl-CoA C-acetyltransferase	Metabolic	2.0 accoa_c ⇌ aacoa_c + coa_c
phaB	Acetoacetyl-CoA Reductase	Metabolic	aacoa_c + h_c + nadph_c ⇌ hbcoa__3R_c + nadp_c
phaC	PHA Synthase Subunit PhaC	Metabolic	hbcoa__3R_c ⇌ coa_c + phb_c
–	–	Demand	phb_c →

Gene indicates the name of the gene responsible for carrying out the metabolic reaction in the model. *Reaction Name* refers to name of the reaction added to the model. *Reaction Type* indicates whether the added reaction is an exchange reaction, which allows metabolites to flow in or out of the system, a transport or reaction, which allows metabolites to flow between the extracellular, periplasmic, and cytosolic compartments, or a metabolic reaction, which produces new output metabolites from inputs. *Reaction Equation* contains the metabolites that are involved in the metabolic reaction. Full names for metabolite abbreviations are as follows: phleth is styrene, atp is ATP, h2o is water, adp is ADP, fadh2 is $FADH_2$, pi is phosphate, fad is FAD, h is hydrogen, phloxi_s2 is (S)-2-phenyloxirane, pacald is phenylacetaldehyde, accoa is acetyl-CoA, aacoa is acetoacetyl-CoA, coa is CoA, nadph is NADPH, nadp is NADP, hbcoa__3R is (R)-3-Hydroxybutanoyl-CoA, and phb is PHB. Metabolites are appended with '_e', '_p', or '_c' to indicate that they are from the extracellular, periplasmic, or cytosolic compartment, respectively.

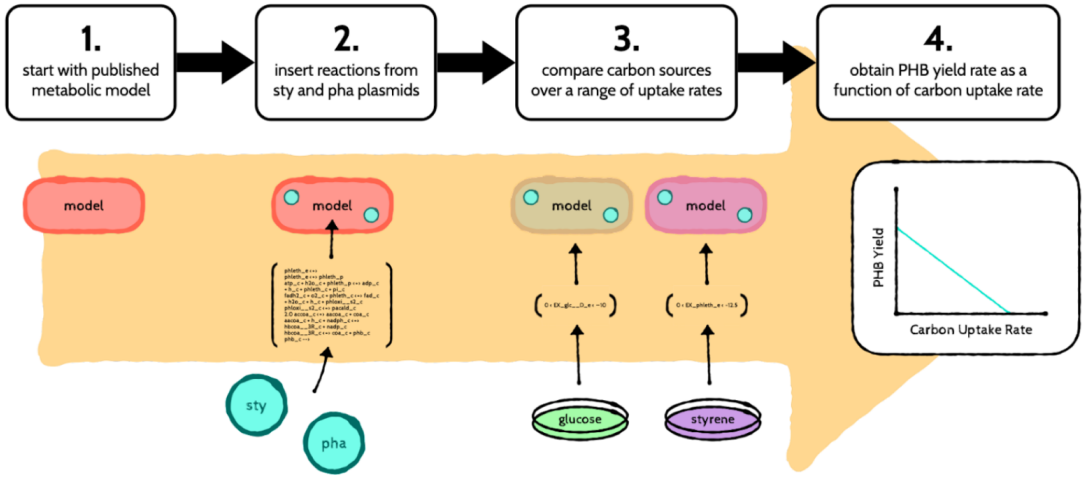

Supplemental Fig. 3. Illustration of Robustness Analysis Timeline. Using a previously published model for *E. coli*, IML1515, all relevant reactions for the sty and pha plasmids were added to the model to better reflect our sponsor's strain of bacteria. Robustness analysis was then performed to compare PHB yield over a range of carbon uptake rates on styrene-based and glucose-based feedstocks.

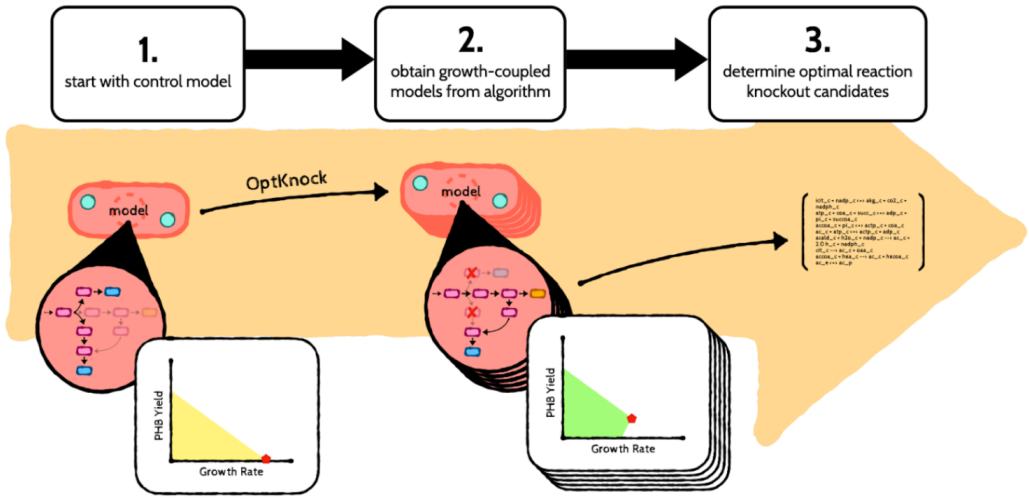

Supplemental Fig. 4. Illustration of OptKnock Analysis Timeline. The control metabolic model produced earlier is inputted into the OptKnock algorithm, which attempts to couple PHB production to growth in the model. A list of optimal reaction knockout candidates is determined from the results.

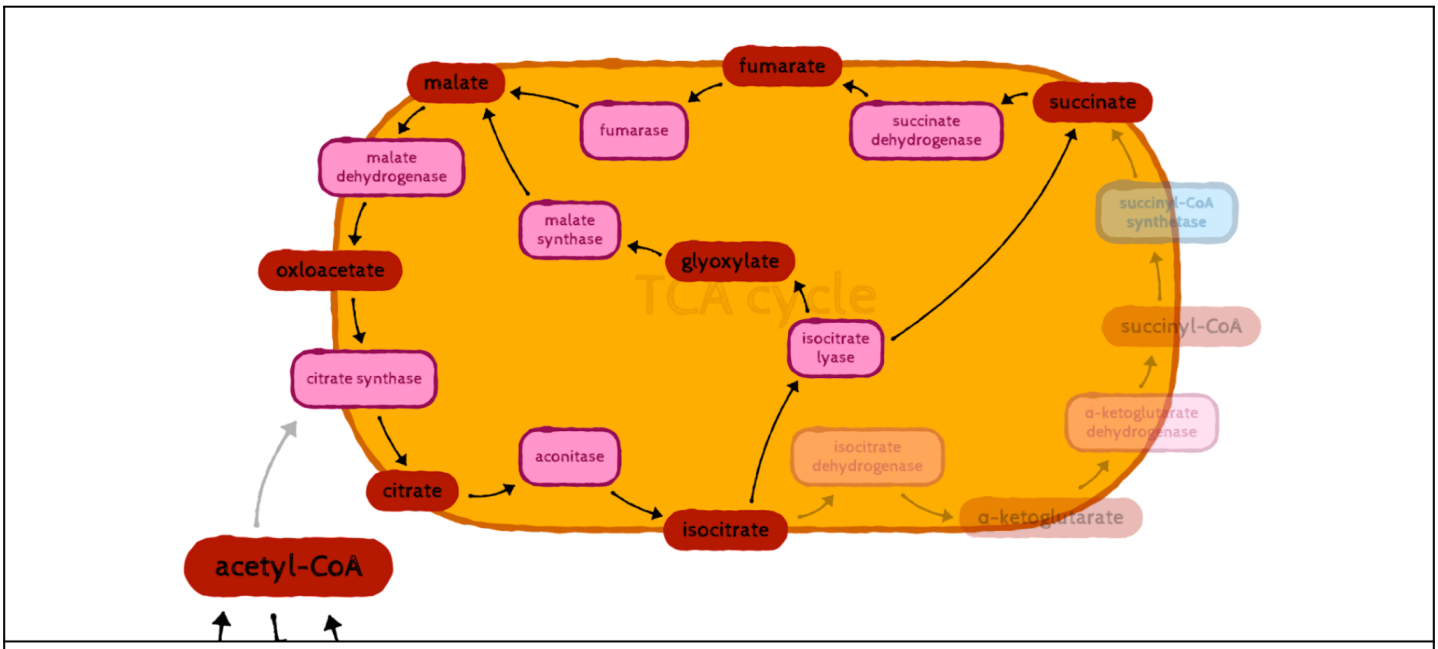

Supplemental Fig. 5. Illustration of Succinyl-CoA Synthetase Knockout Inducing Activation of Glyoxylate Shunt. The glyoxylate shunt bypasses the aerobic portion of the TCA cycle headed by succinyl-CoA synthetase, and prevents carbon loss as carbon dioxide in the TCA cycle.